Chinese Journal of
POLYMER SCIENCE

RESEARCH ARTICLE

https://doi.org/10.1007/s10118-023-3008-1
Chinese J. Polym. Sci. **2023**, *41*, 1591–1598

Contact Electrification Spectrum for Performance Enhancement Mechanism Investigation of Triboelectric Nanogenerators based on Silicone Elastomers with Different Surface Microstructures

Jianliang Gong[a], Shenyang Ye[a], Yan Luo[a], Liqiong Xia[a], Bingyu Liu[a], and Yiwang Chen[a,b*]

[a] *National Engineering Research Center for Carbohydrate Synthesis/Key Laboratory of Fluorine and Silicon for Energy Materials and Chemistry of Ministry of Education, College of Chemistry and Chemical Engineering, Jiangxi Normal University, Nanchang 330022, China*
[b] *Institute of Polymers and Energy Chemistry (IPEC) / Jiangxi Provincial Key Laboratory of New Energy Chemistry, Nanchang University, Nanchang 330031, China*

Electronic Supplementary Information

Abstract Triboelectric nanogenerators (TENGs) based on conjunctive effects of contact electrification (CE) and electrostatic induction are emerging as a new mechanical energy harvesting and sensing technique for promising applications in smart wearables, Internet of Things (IoTs), *etc*. The surface microstructure of a flexible triboelectric material for the increase of surface area is a common strategy for performance enhancement of TENGs, but the real roles of surface microstructures on their output performance are still not explicit due to the lack of suitable analysis tool and rational experimental design. Taking advantages of the surface-sensitive characteristic of CE effect, this work exploited and developed the electric signal patterns generated by single impact of TENGs as a kind of CE spectrum to analyze and speculate the real roles of surface microstructures of flexible triboelectric materials on the output performance of TENGs. Firstly, four different kinds of surface microstructures, namely planar surface (PS) and three combinations of two basic surface microstructures, *i.e.*, micro lens arrays (MLAs), fabric textures (FTs), and hierarchical structures of MLAs on FTs (MLA/FTs), were elaborately designed and introduced for an identical triboelectric material (*i.e.*, silicone elastomer) by a (micro)molding synthesis route. Then they were used for assembly of TENGs based on vertical contact mode to conduct performance evaluation under the same triggering conditions. Through systematic analysis and comparison of their highly repeatable CE spectra by programmed machine, it was found that the surface microstructure for a flexible triboelectric material to maximally enhance the output performance of a TENG shall achieve a positive synergistic effect of increasing triboelectric charge density, effective contact area and contacting/separating velocity, rather than simple increase of its surface area.

Keywords Contact electrification spectrum; Silicone elastomer; Surface microstructures; Triboelectric nanogenerators; Enhancement mechanism

Citation: Gong, J.; Ye, S.; Luo, Y.; Xia, L.; Liu, B.; Chen, Y. Contact electrification spectrum for performance enhancement mechanism investigation of triboelectric nanogenerators based on silicone elastomers with different surface microstructures. *Chinese J. Polym. Sci.* **2023**, *41*, 1591–1598.

INTRODUCTION

Contact electrification (CE) is a well-known phenomenon involving a complex process that occurs commonly between two physical contacting/separating materials.[1−5] The transfer of electrons, ions and/or molecules is regarded to occur when two materials contact closely (such as at the interatomic distance, typically ~0.2 nm), leading to the generation of opposite but equal triboelectric charges on the mutually contact regions after separation.[4,6−8] CE is usually regarded as a negative effect that should be avoided in daily life and industrial production because it can result in dangerous instantaneous discharge, electrical fire and energy losses. It has also been explored for some positive applications, such as electrophotography, electrostatic self-assembly and facile fabrication of electrostatically charged air filters.[9−12] Recently, through skillful lamination of electrodes on the noncontact surface of two materials, CE is coupled with the effect of electrostatic induction for a novel kind of triboelectric nanogenerators (TENGs), which can effectively convert random, low-frequency and broadly distributed ambient mechanical energy to electricity in a clean, green and sustainable process.[13−18] In addition, because of economical and abundant resources of triboelectric materials, simple fabrication procedures, TENGs are emerging as a new kind of sustainable mechanical energy-driven electric generators like existed ambient energy harvesters (such as photovoltaic cells, thermoelectric module and piezoelectric nanogenerators) with huge potentials as either distributed and portable power supply for driving wireless portable/wearable electronics with small operation power or integrated installation

* Corresponding author, E-mail: ywchen@ncu.edu.cn

Special issue: Celebrating the 70th Anniversary of the Establishment of Polymer Program at Peking University
Received March 29, 2023; Accepted May 30, 2023; Published online July 5, 2023

as power plant for electric generation in large scale without occupation of limited space and land.[19–22]

Different from the body charge (electron) generation and transport of most ambient energy harvesting devices, the key process of generating and transferring electrons and/or charges of TENGs occurs at the contacting surfaces of two triboelectric materials.[7,8] To create strong CE effects for high electric generation performance, triboelectric materials with high tendency of being negatively/positively charged are often selected for TENG assembly, such as fluorinated polymers and silicone elastomers (SEs).[23,24] In addition, owing to easier and more versatile processability, SE has been developed as one of the most frequently-used triboelectric materials to design and fabricate various kinds of lightweight and/or flexible TENG devices for a wide range of mechanical energy harvesting and sensing applications.[25–32] Over the past decade, considerable efforts have also been devoted on the development of SEs with controllable surface microstructures for further performance enhancement of TENGs.[28–32] The reported TENGs based on patterned SE surfaces generally show a higher output performance than TENGs with a planar surface of SEs. The main reason is often simply ascribed to the increase of surface (contact) area. There are few reports on further elucidating the real roles and impacts of surface morphology on the output performance of TENGs. Due to different surface microstructures, triboelectric material pairs and triggering conditions, it is also difficult to speculate the performance enhancement mechanism of surface microstructures for TENGs by conducting systematic comparison and analysis based on the reported literatures.

In the past decade, we devoted ourselves to understanding the origin of CE phenomena to enable the controllable generation of electrostatic charges and mechanoradicals for rational design and assembly of mechanical energy management devices for green, sustainable and highly-effective utilization of the mechanical energy that broadly exists but is wasted in the environment.[16,17,30,33–35] For the first time, the formation reasons of both mechanoradicals and electrostatic charges were explicitly elucidated in one direct chemical bond cleavage mechanism mode by the combination of polymer chain entanglement, bond dissociation energy with nucleophilic substitution reaction based on a special viscoelastic polymer adhesive as CE material. Considering the occurrence of CE in an open environment, we further find the existence of ambient substances, such as water and oxygen, can spark a series of chain reactions for the new generation of macromolecular charges and radicals, leading to a strong electrostatic phenomenon and mechanoradical chemical reaction that can be observed macroscopically. These new, thorough and more comprehensive CE understandings are keys to obtain triboelectric materials with high charge densities through the optimal choices of CE pairs and triggering conditions, while the charge density was demonstrated to be the single most important influencing factor that has the highest-order effect on the output performance of TENGs as a kind of electric generators in our previous work.[35] The different charge generation, transfer, and accumulation processes under different CE triggering conditions facilitate the generation of different electric signal, also allowing TENGs to function as self-powered sensors. Through systematically investigating the influences of triggering conditions (*i.e.*, impact forces and frequencies) on the electrical signals (*i.e.*, output voltage and charge density), we successfully developed various kinds of flexible and wearable TENGs as self-powered interactive textiles and highly integrable mechanical energy sensing units with tailorable sizes and shapes to detect and monitor the body motions of human beings at different work and life scenarios.[33–35]

In this work, four different kinds of TENGs were designed and fabricated based on an identical triboelectric material (*i.e.*, silicone elastomer) with planar surface (PS) and three combinations of two basic surface microstructures, *i.e.*, micro lens arrays (MLAs), fabric textures (FTs), and hierarchical structures of MLAs on FTs (MLA/FTs), respectively. Their output performances were strictly evaluated by a programmed machine under the same triggering conditions. The electric signal patterns by single triggering cycle (*i.e.*, CE spectrum) were particularly compared and analyzed to better understand the roles of surface morphology on the output performance of TENGs.

EXPERIMENTAL

Materials

SYLGARD™ 184 silicone elastomer (SE) kit (two-part, 10 to 1 mix ratio) was purchased from the Dow Chemical Company. Poly(dimethylsiloxane)-graft-polyacrylates (PDMS-*g*-PAs, M_n ~26000, dimethylsiloxane composition, ~80 wt%) and chloroform ($CHCl_3$, anhydrous, ≥99.9%) were purchased from Sigma-Aldrich, Ltd. Copper/nickel coated polyester fabric (CNF) was brought from 3M Corp. All materials were used as received without further purification.

Design and Fabrication of (Micro)Molds with Different Surface Microstructures

Commercially available glass sheets and CNFs were directly used as molds with planar surface (PS) and fabric surface (FS), respectively. To prepare micromolds with honeycomb porous surface (HPS), a unique bottom-up strategy of using water droplets (*i.e.*, breath figure (BF) strategy) was employed by simply drying a continuous polymer solution film on a PS substrate in a high-humidity environment at room temperature. The relative humidity was over 90%. The used polymer solution was prepared by dissolving PDMS-*g*-PAs in $CHCl_3$ at the concentration of 15 mg·mL^{-1}. Through the quick evaporation of low-boiling-point solvent $CHCl_3$, the surface temperature of solution film dropped quickly to induce the nuclei and growth of water droplets as spherical shapes. The condensed water acted as nonsolvents to induce the aggregation of polymers at the nonsolvent/solution interface to stabilize the formed droplets. The isolated spherical droplets can further self-assemble into hexagonal arrays driven by the surface convection and capillary attractive force. With continuous evaporation of solvent, this BF process involving self-assembly of both water droplets and polymers was regarded as termination after gelation/solidification occurs. The substrate was taken out for air drying to further remove residual water and solvent. And polymers were left on the PS substrate as HPS microstructures. The same BF procedures was employed to

https://doi.org/10.1007/s10118-023-3008-1

prepare micromolds with hierarchical structures of HPS 3D conformably formed on FS (HPS/FS). The PS substrate was simply replaced by a planar substrate adhered with a piece of CNF.

(Micro)Molding Fabrication of SE Films with Different Surface Microstructures

Four kinds of (micro)molds with PS, HPS, FS and HPS/FS were used for templating fabrication of SE films with corresponding patterns, respectively. The used SYLGARD 184 SE was supplied in a kit consisting of base and curing agent in separate containers. Before use, the base and curing agent were homogeneously mixed at a weight ratio of 10:1. Fig. S2 (in the electronic supplementary information, ESI) schematically illustrated an example of micromolding fabrication of SE film with a hierarchical structural surface features of micro lens arrays and fabric textures (MLA/FT) from a substrate with FS. A kind of micromolds with hierarchical structures of HPS/FS (Figs. S2b and S2f, in ESI) was firstly prepared from FS (Figs. S2a and S2e in ESI) by the BF strategy stated above. Then the well mixed SE precursors were cast on the HPS/FS micromold according to the mass-to surface-area ratio of 0.048 $g\cdot cm^{-2}$ by a doctor-blading method. It was further shifted to a vacuum oven for de-airing at room temperature. After de-airing for 30 min, the oven temperature was increased to 80 °C for 2 h to cross-link SE precursors for a cured film (Fig. S2c in ESI). Finally, the cured SE film was peeled off from the micromold carefully, possessing a hierarchical structural surface of MLA/FTs (Figs. S2d and S2g in ESI).

Assembly of Machine-driven TENG Device to Investigate the Influence of Surface Microstructures of Triboelectric Materials on the Output Performance

A TENG device with a 10 mm × 10 mm copper sheet fixed as one triboelectric material was used to investigate the influence of surface microstructures of SE films on the output performance. The copper sheet also played an electrode role. It was adhered to an insulating impact plate that can be driven by a Keyboard Life Tester (ZX-A03) at a continuous dynamic sinusoidal motion with a maximum displacement of 10 mm using controllable impact force and frequency. The SE film of 20 cm^2 (greatly larger than copper sheet) was used as another triboelectric material. When tested, it was fixed by adhering its smooth surface to a conductive adhesive laminated on an insulating bottom substrate. Its surface patterned with desired microstructures was used for CE with copper sheet *via* a repetitively impact process at 100 N and 3 Hz. An oscilloscope (Keisight DSO-X3014A) with a high voltage probe (Keisight N2790A) was connected to the copper electrode and conductive adhesive electrode respectively for monitoring the variations of electric signals during the impact process. After impacting 15 min to achieve the saturation of triboelectric charges on the dielectric surface of triboelectric materials, the output voltages across a load with an equivalent resistance of 8 MΩ were measured for further quantitative analysis.

RESULTS AND DISCUSSION

Fig.1 shows the (micro)molding fabrication routes for different surface microstructures using an identical triboelectric material. Firstly, four kinds of (micro)molds with planar surface (PS, Fig. 1a), honeycomb porous surface (HPS, Fig. 1b), fabric surface (FS, Fig. 1c), and three-dimensionally HPS conformably formed on nonplanar FS (HPS/FS, Fig. 1d) were prepared based on our previous reports (For details, see ESI, Figs. S1 and S2 in ESI).[33,34,36,37] Silicone (SE) is one of the most broadly-used triboelectric materials for TENGs owing to its excellent electronegativity for high tendency of being negatively charged and wide processing conditions for easy fabrication of desired structures *via* various techniques. Herein, it was selected as the triboelectric material to fabricate SE films with controllable surface microstructures by directly casting its precursors onto the corresponding (micro)molds. After vacuum degassing and cross-linkage, the solidified SE films were peeled off from the micromolds, leading to PS structures (Fig. 1e), MLA microstructures (Fig. 1f), FT microstructures (Fig. 1g) and MLA/FT hierarchical microstructures (Fig. 1h), respectively (For more details, see ESI and Fig. S2 in ESI). Figs. 1(i)−1(l) show their typical surface morphologies, and their cross-sectional views were displayed in Figs. 1(m)−1(p), respectively. The micro lens size, height and density of MLA films were approximately 2.57 μm, 0.35 μm, and 2.45×10^7 cm^{-2}, respectively. The single fiber channel size of FT films was 15.67 μm (width) and 5.90 μm (depth), respectively. Comparing to planar surface area, the surface area of SE films surface engineered with MLAs, FTs and MLA/FTs increased approximately 36.2%, 38.9% and 49.2%, respectively (For details, see ESI and Fig. S3 in ESI).

Fig. 2(a) illustrates the TENG device to obtain CE spectrum for quantitative performance evaluation of triboelectric materials with different surface microstructures (For details, see ESI). A 10 mm × 10 mm copper sheet with a maximum separation distance of 10 mm was used to impact SE film repetitively. Its operational principle of converting mechanical energy to electricity was generally regarded to be the conjunctive effects of CE and electrostatic induction.[13−15,35] As schematically shown in Fig. 2(b-iii), CE enables the generation of opposite triboelectric charges on the contact area of two materials through repetitive contact, respectively. After separation, it leads to establish a potential difference between the two electrodes under an open-circuit condition. When shorting the electrodes or connecting an external load between them, the potential difference is balanced by neutralizing the positively charged surface of copper sheet with the electrons from the electrode laminated with the negatively charged SE film. At the static separation state, the negative triboelectric charges retain on the dielectric surface of SE film, while the electrode is positively charged based on electrostatic induction effect (Fig. 2b-i). During the contacting and separating process, free electrons are driven to flow forth (Fig. 2b-ii) and back (Fig. 2b-iv) between the electrodes to build an opposite potential to combat against the dynamic potential field for electrostatic balance. These two processes lead to the formation of an alternating current. The output voltages across an external load with equivalent resistance of 8 MΩ were collected after repetitively impacting the SE surface with copper sheet for 15 min at 100 N and 3 Hz with an impact velocity of 0.059 $m\cdot s^{-1}$. Figs. 2(c)−2(f) show the typical output voltage curves generated by SE films with PS, MLA, FT, and MLA/FT, respectively. Their electric signals triggered by a single impact cycle involving contact and separation are magnified and shown in Figs. 2(g)−2(j), respectively. They all show a pair

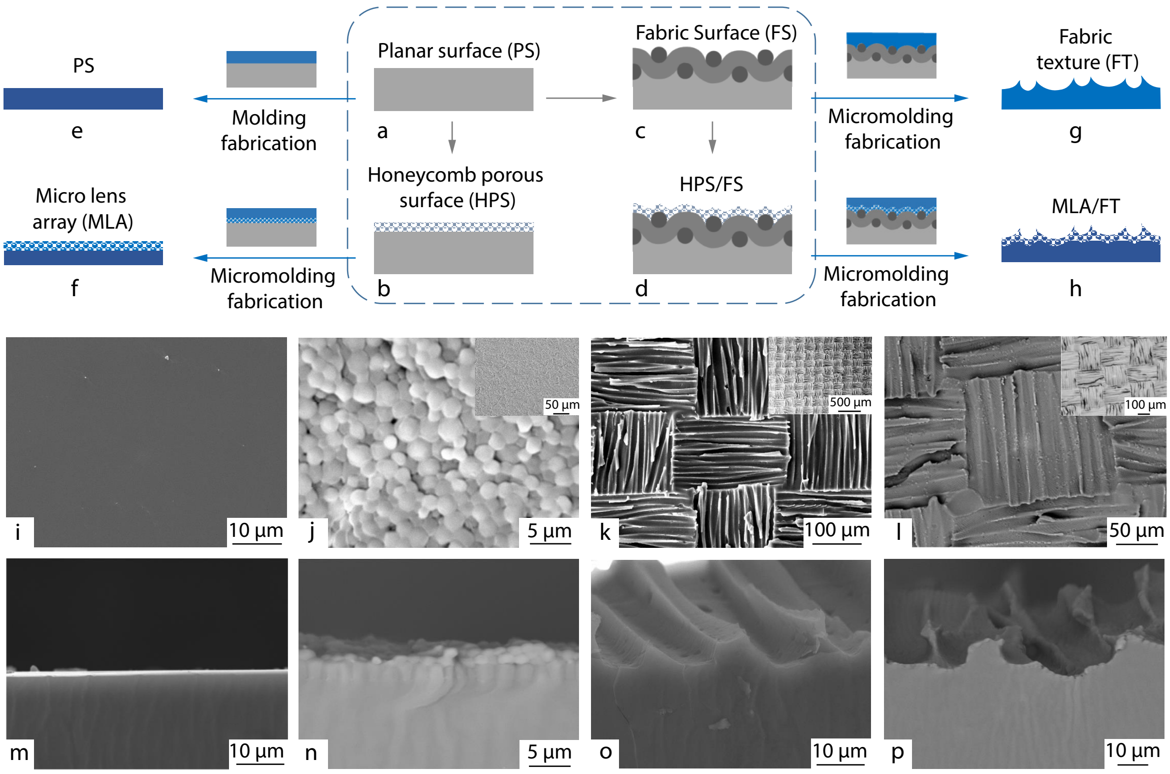

Fig. 1 Schematics of (micro)molding fabrication routes for different surface microstructures using an identical triboelectric material, *i.e.*, silicone elastomer (SE): SE films with (e) PS structures molded from (a) planar substrate, (f) MLAs micromolded from (b) and HPS film, FTs micromolded from (c) FS film, and (h) hierarchical structures of MLA/FTs micromolded from HPS/FS film. Typical top views of (i) PS, (j) MLAs, (k) FTs, and (l) MLA/FTs. Typical cross-sectional views of (m) PS, (n) MLAs, (o) FTs and (p) MLA/FTs. The insets of (j), (k) and (l) are typical images of MLAs, FTs and MLA/FTs at low magnification, respectively.

of positive and negative peaks, which were generated during the contacting and separating process of an impact cycle, respectively. Here this kind of electric signal patterns triggered by a single full impact cycle involving separation, contacting, contact, and separating was defined as CE spectrum (or triboelectric spectrum). The obtained CE spectra generated by all SE samples were highly repeatable (Fig. S4 in ESI), indicating the robustness of the proposed TENG device used to collect electric signals for quantitative performance analysis and comparison of different triboelectric materials.

Fig. 3(a) further stacks the typical CE spectra generated by SE films with four different surface microstructures for more explicit comparison and detailed analysis. All SE film surface morphologies resulted in the formation of multiple peaks. The positive peaks generated during the contacting process were identified with numerical order from left to right, while the negative peaks generated during the separating process were identified using alphabetical order from right to left. It was obvious MLA/FT and FT generated more positive and negative peaks than PS and MLA. Fig. 3(b) summarizes their maximum peak voltages. The maximum peak voltages generated by FTs were the highest, followed by MLA/FTs, PS and MLA. Its negative peak voltage was also the highest, but the voltage of PS negative peak became larger than that of MLA/FTs. MLA still generated the smallest negative peak voltage. The time intervals between the maximum positive peak and negative peak for different surface microstructures are shown in Fig. 3(c). It shows a consistent variation trend with the negative peak voltage generated during the separating process. A larger time interval led to a higher voltage of negative peak. It shall be noted that MLAs should show the second-best output performance because of its second-largest surface area. Moreover, based on the surface areas of four different surface microstructures stated above, the output performance shall be sorted as MLA/FTs > FTs–MLAs > PS. These results indicate that the output performance of SE films is not simply dependent on the surface areas of triboelectric materials.

The main reasons for generation of multiple peaks were usually ascribed to be the complex impacting conditions.[38,39] Essentially, they may be due to the successive contact or separation of different local regions of two CE surfaces. The surface of a SE film can be regarded to be consisted of numerous electrostatically charged regions of nanoscopic dimensions.[7,8] During the contacting/separating process, it is impossible to achieve full contact/separation for the surfaces of two triboelectric materials synchronously. The final CE spectra were constituted of electric signals generated by different contacting/separating local regions. These electric signals were highly sensitive to their distances, and this electric generation process was demonstrated theoretically and experimentally to occur within a very close distance, *e.g.*, less than 1 mm when the impacting velocity is 0.10 $m\cdot s^{-1}$.[38] The unimodal peak signal would be splitted into two or more peaks

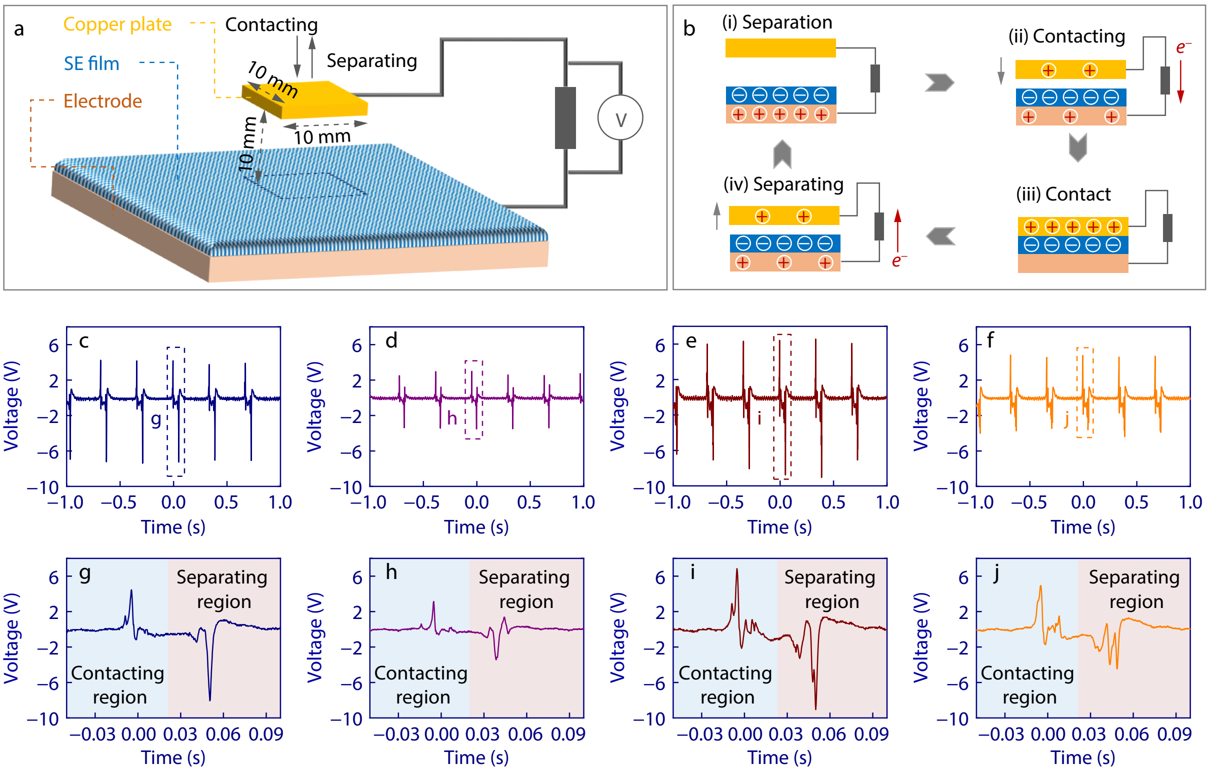

Fig. 2 Schematics of (a) a TENG device and (b) its operational principle to obtain CE spectrum for output performance evaluation of triboelectric materials. Typical output voltage curves of SE films with (c) PS, (d) MLAs, (e) FTs, and (f) MLA/FTs; Typical CE spectra of SE films with (g) PS, (h) MLAs, (i) FTs, and (j) MLA/FTs triggered by an impact cycle under the same triggering conditions.

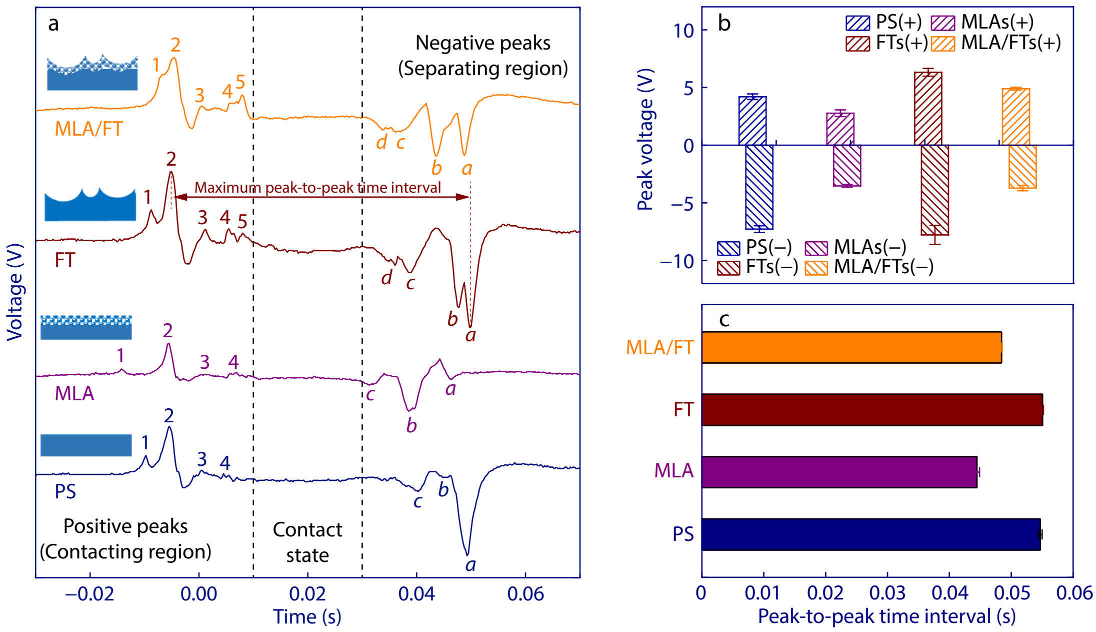

Fig. 3 The influences of surface microstructures on (a) CE spectra, (b) maximum peak voltages, and (c) time intervals between maximum positive peak and maximum negative peak.

when the distances among the contacting/separating local regions with considerable areal size had distinct differences. Therefore, the more peaks generated by MLA/FTs and FTs can be ascribed to their more asynchronized contacting/separating local regions, because of the larger and more various height differences of microstructural regions.

The electric performance of TENGs shall be mainly determined by the triboelectric charge density of dielectric materials and effective contacting area between two CE surfaces when fixing the same triggering conditions (*i.e.*, applied force and

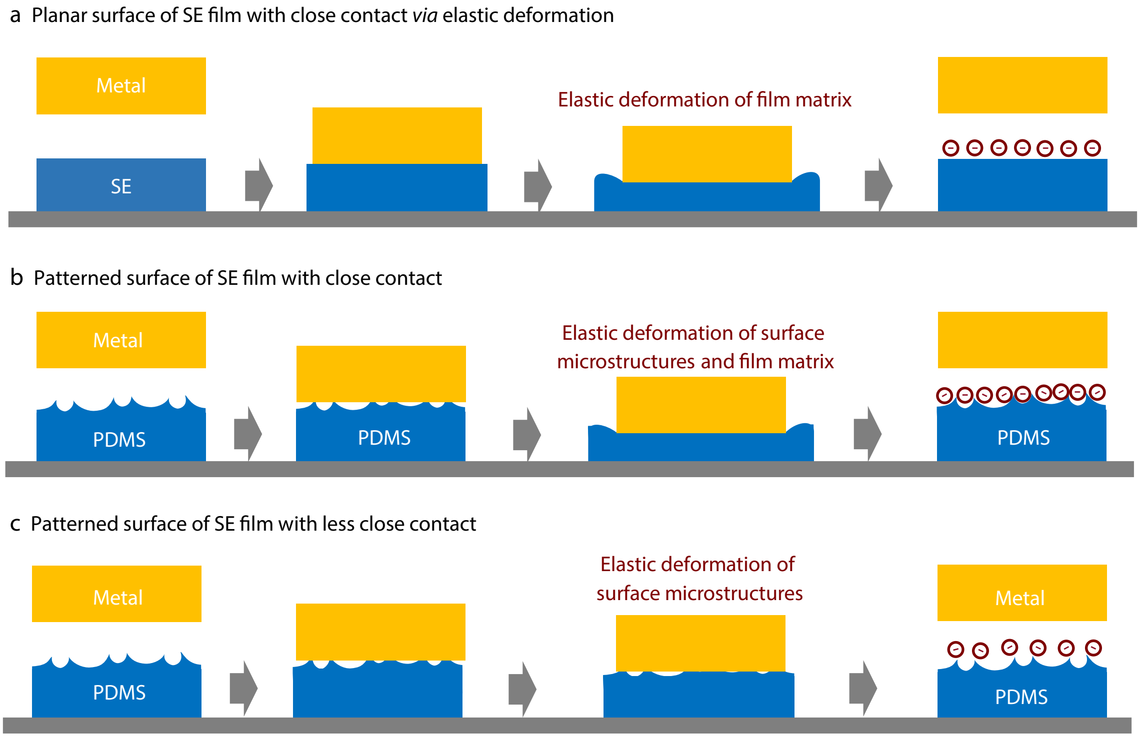

Fig. 4 The influence of surface microstructures of SE films on the effective contact area during the CE process under different applied forces, (a) close contact *via* elastic deformation of SE film matrix, (b) close contact *via* elastic deformation of both surface microstructures and film matrix of SE, (c) less close contact *via* only elastic deformation of SE surface microstructures.

frequency). They should be both increased by the surface microstructures of a flexible/soft triboelectric materials (*i.e.*, SE) for a kind of output performance-enhanced TENGs. The elastic surface of a SE film contributes to more effective contact regions (contact intimacy) with another triboelectric material *via* elastic deformation (Fig. 4a) for higher triboelectric charge density, while the introduction of surface microstructures leads to higher surface area with the expectation of further increase of effective contact area (Fig. 4b). However, if the applied external force was too small to render the elastic deformation of surface microstructures, numerous air microgaps may be left between two CE surfaces, resulting in the decrease of effective contact area, rather than increasing with the increase of surface area (Fig. 4c). Therefore, the output performance (*i.e.*, output voltage) of SE film-based TENGs does not show a consistent increase trend with the increase of surface area. When the SE film was replaced with a polymer film without surface elasticity (such as polytetrafluoroethylene) and impacted by hard metallic fabric surface and hard metallic planar surface, respectively, it was found the former output performance showed a significant decrease comparing to the latter (Fig. S5 in ESI). The main reason can be ascribed to the decrease of effective contact area for triboelectric charge generation caused by hard patterns.

Besides surface area, the different time intervals between the maximum positive peak and negative peak indicate that the microstructures of SE surface may also slightly influence the contacting/separating velocity of another triboelectric surface. We have experimentally and theoretically verified that the output voltage of TENGs based on vertical contact-separation mode showed a monotonic increase with the increase of impact velocity.[35,38] It was also found that, at a higher impact velocity, the separation distance required for achieving the maximum peak voltage became larger. Because the impact velocity controlled by the programmed machine was identical for all testing samples, the different maximum peak-to-peak time intervals determined by both separating velocity and separation distance can be ascribed to the different surface microstructures of SE films. The viscoelastic surface of SE film plays a cushioning role during the contacting process for positive peak generation, while it may accelerate the separating process *via* resilience force for negative peak generation. This can be reflected from the negative peak signals in the CE spectrum, which are generally larger than their corresponding positive peak voltages. The larger time interval between positive and negative peaks indicates a larger separation distance to achieve the maximum voltage of negative peak, which also suggests a longer effective electricity generating time. The increase of time interval can be inherently ascribed to the enhancement of electrostatic filed caused by the increase of triboelectric charge density. Therefore, both positive and negative peak voltages show an increase trend with the increase of peak-to-peak time intervals. The best output performance generated by SE film with FTs surface features can be ascribe to its unique elastic surface microstructures that can achieve a positive synergistic effect among triboelectric charge density, effective contact area and separating velocity under the specific CE conditions with copper sheet.

CONCLUSIONS

In conclusion, we developed and demonstrated a new spectrum technique, namely CE spectrum generated by single impact of TENGs (acting as CE spectrometer), to analyze and speculate the real roles of surface microstructures of flexible triboelectric materials on the output performance of TENGs. Four different kinds of surface microstructures (*i.e.*, PS, MLA, FTs and MLA/FTs) with elaborate design were successfully introduced for an identical triboelectric material by a (micro)molding synthesis route and used for assembly and performance optimization of vertical contact mode based TENGs under the same triggering conditions. Through systematic analysis and comparison of their highly repeatable CE spectrums by programmed machine, it was found that the surface microstructure for a flexible triboelectric material to maximally enhance the output performance of a TENG shall achieve a positive synergistic effect of increasing both triboelectric charge density/effective contact area and contacting/separating velocity, rather than simple increase of its surface area.

Conflict of Interests

The authors declare no interest conflict.

Electronic Supplementary Information

Electronic supplementary information (ESI) is available free of charge in the online version of this article at http://doi.org/10.1007/s10118-023-3008-1.

ACKNOWLEDGMENTS

This work was financially supported by the National Natural Science Foundation of China (No. 52103278).

REFERENCES

1 Lowell, J.; Rose-Innes, A. C. Contact electrification. *Adv. Phys.* **1980**, *29*, 947.
2 Horn, R. G.; Smith, D. T. Contact electrification and adhesion between dissimilar materials. *Science* **1992**, *256*, 362–364.
3 Horn, R. G.; Smith, D. T.; Grabbe, A. Contact electrification induced by monolayer modification of a surface and relation to acid-base interactions. *Nature* **1993**, *366*, 442–443.
4 McCarty, L. S.; Whitesides, G. M. Electrostatic charging due to separation of ions at interfaces: contact electrification of ionic electrets. *Angew. Chem. Int. Ed.* **2008**, *47*, 2188–2207.
5 Lacks, D. J.; Sankaran, R. M. Contact electrification of insulating materials. *J. Phys. D: Appl. Phys* **2011**, *44*, 453001.
6 Wang, Z. L.; Wang, A. C. On the origin of contact-electrification. *Mater. Today* **2019**, *30*, 34–51.
7 Baytekin, H. T.; Patashinski, A. Z.; Branicki, M.; Baytekin, B.; Soh, S.; Grzybowski, B. A. The mosaic of surface charge in contact electrification. *Science* **2011**, *333*, 308–312.
8 Baytekin, H. T.; Baytekin, B.; Hermans, T. M.; Kowalczyk, B.; Grzybowski, B. A. Control of surface charges by radicals as a principle of antistatic polymers protecting electronic circuitry. *Science* **2013**, *341*, 1368–1371.
9 Grzybowski, B. A.; Winkleman, A.; Wiles, J. A.; Brumer, Y.; Whitesides, G. M. Electrostatic self-assembly of macroscopic crystals using contact electrification. *Nat. Mater.* **2003**, *2*, 241–245.
10 Kalsin, A. M.; Fialkowski, M.; Paszewski, M.; Smoukov, S. K.; Bishop, K. J. M.; Grzybowski, B. A. Electrostatic self-assembly of binary nanoparticle crystals with a diamond-like lattice. *Science* **2006**, *312*, 420–424.
11 Bai, Y.; Han, C. B.; He, C.; Gu, G. Q.; Nie, J. H.; Shao, J. J.; Xiao, T. X.; Deng, C. R.; Wang, Z. L.; Washable multilayer triboelectric air filter for efficient particulate matter PM2.5 removal. *Adv. Funct. Mater.* **2018**, *28*, 1706680.
12 Liu, J. Q.; Jiang, T.; Li, X. H.; Wang, Z. L. Triboelectric filtering for air purification. *Nanotechnology* **2019**, *30*, 29.
13 Fan, F. R.; Tian, Z. Q.; Wang, Z. L. Flexible triboelectric generator. *Nano Energy* **2012**, *1*, 328–334.
14 Wang, Z. L. Triboelectric nanogenerators as new energy technology and self-powered sensors-principles, problems and perspectives. *Faraday Discuss.* **2014**, *176*, 447–458.
15 Zhu, G.; Peng, B.; Chen, J.; Jing, Q. S.; Wang, Z. L. Triboelectric nanogenerators as a new energy technology: from fundamentals, devices, to applications. *Nano Energy* **2015**, *14*, 126–138.
16 Gong, J. L.; Xu, B. G.; Yang, Y. J.; Wu, M. J.; Yang, B. An adhesive surface enables high-performance mechanical energy harvesting with unique frequency-insensitive and pressure-enhanced output characteristics. *Adv. Mater.* **2020**, *32*, 1907948.
17 Gong, J. L.; Xu, B. G.; Guan, X. Y.; Chen, Y. J.; Li, S. Y.; Feng, J. Towards truly wearable energy harvesters with full structural integrity of fiber materials. *Nano Energy* **2019**, *58*, 365–374.
18 Xu, W. H.; Zheng, H. X.; Liu, Y.; Zhou, X. F.; Zhang, C.; Song, Y. X.; Deng, X.; Leung, M.; Yang, Z. B.; Xu, R. X.; Wang, Z. L.; Zeng, X. C.; Wang, Z. K. A droplet-based electricity generator with high instantaneous power density. *Nature* **2020**, *578*, 392–396.
19 Shi, J. D.; Liu, S.; Zhang, L. S.; Yang, B.; Shu, L.; Yang, Y.; Ren, M.; Wang, Y.; Chen, J. W.; Chen, W.; Chai, Y.; Tao, X. M. Smart textile-integrated microelectronic systems for wearable applications. *Adv. Mater.* **2020**, *32*, 1901958.
20 Tao, X. M. Study of fiber-based wearable energy systems. *Acc. Chem. Res.* **2019**, *52*, 307–315.
21 Wang, Z. L.; Jiang, T.; Xu, L. Toward the blue energy dream by triboelectric nanogenerator networks. *Nano Energy* **2017**, *39*, 9–23.
22 Chen, H.; Xing, C.; Li, Y. L.; Wang, J.; Xu, Y. Triboelectric nanogenerators for a macro-scale blue energy harvesting and self-powered marine environmental monitoring system. *Sustain. Energy Fuels* **2020**, *4*, 1063–1077.
23 Zou, H.; Zhang, Y.; Guo, L.; Wang, P.; He, X.; Dai, G.; Zheng, H.; Chen, C.; Wang, A. C.; Xu, C.; Wang, Z. L. Quantifying the triboelectric series. *Nat. Commun.* **2019**, *10*, 1427.
24 Liu, S. R.; Zheng, W.; Yang, B.; Tao, X. M. Triboelectric charge density of porous and deformable fabrics made from polymer fibers. *Nano Energy* **2018**, *53*, 383–390.
25 Dong, K.; Deng, J. N.; Zi, Y. L.; Wang, Y. C.; Xu, C.; Zou, H. Y.; Ding, W. B.; Dai, Y. J.; Gu, B. H.; Sun, B. Z.; Wang, Z. L. 3D orthogonal woven triboelectric nanogenerator for effective biomechanical energy harvesting and as self-powered active motion sensors. *Adv. Mater.* **2017**, *29*, 1702648.
26 Xia, X. N.; Chen, J.; Guo, H. Y.; Liu, G. L.; Wei, D. P.; Xi, Y.; Wang, X.; Hu, C. G. Embedding variable micro-capacitors in polydimethylsiloxane for enhancing output power of triboelectric nanogenerator. *Nano Res.* **2017**, *10*, 320–330.

27 Sun, J. G.; Pu, X.; Liu, M. M.; Yu, A. F.; Du, C. H.; Zhai, J. Y.; Hu, W. G.; Wang, Z. L. Self-healable, stretchable, transparent triboelectric nanogenerators as soft power sources. *ACS Nano* **2018**, *12*, 6147–6155.
28 Wang, S. H.; Lin, L.; Wang, Z. L. Nanoscale triboelectric-effect-enabled energy conversion for sustainably powering portable electronics. *Nano Lett.* **2012**, *12*, 6339-6346.
29 Choi, D. S.; Yang, S.; Lee, C.; Kim, W.; Kim, J.; Hong, J. Highly surface-embossed polydimethylsiloxane-based triboelectric nanogenerators with hierarchically nanostructured conductive Ni-Cu fabrics. *ACS Appl. Mater. Interfaces* **2018**, *10*, 33221–33229.
30 Gong, J. L.; Xu, B. G.; Tao, X. M. Breath figure micromolding approach for regulating the microstructures of polymeric films for triboelectric nanogenerators. *ACS Appl. Mater. Interfaces* **2017**, *9*, 4988–4997.
31 Rasel, M. S. U. Park, J. Y. A sandpaper assisted micro-structured polydimethylsiloxane fabrication for human skin based triboelectric energy harvesting application. *Appl. Energy* **2017**, *206*, 150–158.
32 Kim, D. H.; Dudem, B.; Yu, J. S. High-performance flexible piezoelectric-assisted triboelectric hybrid nanogenerator *via* polydimethylsiloxane-encapsulated nanoflower-like ZnO composite films for scavenging energy from daily human activities. *ACS Sustainable Chem. Eng.* **2018**, *6*, 8525–8535.
33 Gong, J. L.; Xu, B. G. 3D conformal surface engineering of continuous fibers with porous microstructures for 1D advanced functional materials. *Macromol. Mater. Eng.* **2021**, *306*, 2000699.
34 Guan, X. Y.; Gong, J. L.; Xu, B. G. Three-dimensional conformal porous microstructural engineering of textile substrates with customized functions of brick materials and inherent advantages of textiles. *ACS Appl. Mater. Interfaces* **2020**, *12*, 17699–17705.
35 Fu, H. Y.; Gong, J. L.; Zhong, H.; Yang, B.; Long, Z. C.; Zeng, J. Q.; Cheng, Z. Y.; He, J. L.; Xu, B. G.; Chen, Y. W. Surface microstructural engineering of silicone elastomers for high performance adhesive surface-enabled mechanical energy harvesters. *J. Mater. Chem. A* **2022**, *10*, 9643–9654.
36 Gong, J. L.; Xu, B. G.; Tao, X. M.; Li, L. Honeycomb microstructured silicon oxycarbide sheets from silicon-containing graft copolymer films. *Plasma. Process. Polym.* **2014**, *11*, 1001–1009.
37 Gong, J. L.; Xu, B. G.; Tao, X. M. Three-dimensionally conformal porous microstructured fabrics *via* breath figures: a nature-inspired approach for novel surface modification of textiles. *Sci. Rep.* **2017**, *7*, 2354.
38 Yang, B.; Zeng, W.; Peng, Z. H.; Liu, S. R.; Chen, K.; Tao, X. M. A fully verified theoretical analysis of contact-mode triboelectric nanogenerators as a wearable power source. *Adv. Energy Mater.* **2016**, *6*, 1600505.
39 Yang, B.; Tao, X. M.; Peng, Z. H. Upper limits for output performance of contact-mode triboelectric nanogenerator systems. *Nano Energy* **2019**, *57*, 66–73.